

---

**COMPARISON OF CRYSTAL SIZE IN DIFFERENT SUPERSATURATION MODES**

Ladislav HLOŽNÝ, Miroslav BROUL and Luděk PROVAZNÍK

*Research Institute of Inorganic Chemistry, 400 60 Ústí nad Labem*

Received October 10, 1990

Accepted January 28, 1991

---

Crystallization of a solution of ammonium aluminium sulfate dodecahydrate by cooling and by vacuum evaporation was performed in a laboratory batch experiment. In the two crystallization modes, the nucleation was found to proceed at different rates whereas the crystal growth rate did not differ significantly.

---

When designing equipment for crystallization from solution, the technologist is often faced with the problem of choosing between cooling and evaporation. For such cases the literature recommends taking into account the temperature dependence of solubility. A number of substances, however, exist where this rule does not lead to unambiguous decision; the choice is then usually made by considering the character of the operations following the crystallization. In the vast majority of cases, cooling crystallization is then intuitively chosen with reference to the fact that this mode requires lower capital and operation costs.

We want to draw attention to another aspect that is often underestimated, viz. the quality of the product. Actually, it is not a matter of course that crystals prepared by cooling and by evaporation should have the same size and purity. In the extreme case it can happen that unsuitable choice of the process will be a source not only of problems in the ensuing operations such as the crystal separation but also of market problems, low-quality crystalline product being difficult to sell.

The effect of the way of supersaturation on the purity of the crystal product for the case of ammonium aluminium sulfate has been discussed recently<sup>1</sup>; the present paper deals with the crystal size emerging from supersaturation by evaporation and by cooling.

**THEORETICAL**

The particle size distribution of crystal products from a continuous mixed suspension-mixed product removal crystallizer (MSMPR) can be described by the relation for the cumulative gamma function<sup>2</sup>

$$M(L) = 100 (1 + z + z^2/2 + z^3/6) \exp(-z) \quad (1)$$

where the dimensionless crystal size  $z$  is

$$z = 3L/L_m \quad (2)$$

the mean crystal size  $L_m$  being defined by

$$L_m = L(M(L_m) = 64.7\%) . \quad (3)$$

Provided that McCabe's  $\Delta L$  rule<sup>3</sup> is obeyed, this mean size of the product crystals in a continuous crystallizer is

$$L_m = 3Gt_1 . \quad (4)$$

The crystal size distribution is a resultant of several simultaneous processes, particularly solution supersaturation, nucleation, and crystal growth. While the way and rate of attaining supersaturation can be chosen within rather wide limits, the nucleation rate and the crystal growth rate depend not only on the conditions chosen, supersaturation in particular, but also on properties of the crystallizing system.

Describing the numerical nucleation rate  $B^0$  and the linear growth rate  $G$  by power type equations,

$$B^0 = k'_N m_c^d \Delta w^n \quad (5)$$

$$G = k'_G \Delta w^g \quad (6)$$

the kinetic parameters of nucleation and crystal growth in a particular system can be combined into the so-called system kinetic constant of crystallization<sup>4</sup>,

$$B_N = 4 \cdot 5^{g/n} k'_G (\alpha \rho_c k'_N)^{g/n} . \quad (7)$$

The following equation can be derived for describing the relation between the mean size of the product crystals  $L_m$  and the continuous crystallizer throughput  $r_c = m_c/t_1$ :

$$L_m^{(1+3i)} = 3B_N m_c^{(1-di)} r_c^{(i-1)} \quad (8)$$

where  $i = g/n$ .

The granulometric composition of products from a discontinuous crystallizer can usually be described satisfactorily also by means of Eq. (1). If the average linear rate of growth in a discontinuous equipment is defined by the equation

$$L_m = Gt_c \quad (9)$$

where  $t_c$  is the time of crystal growth, then the formal relation<sup>5</sup>

$$t_c = 3t_1 \quad (10)$$

follows from a comparison of Eqs (4) and (9). The time  $t_c$  can largely be replaced by the total saturation time  $t_s$ . However, if the starting solution has not been seeded and it has a wide metastable zone, nuclei may appear only after a time comparable to the total time of the experiment  $t_s$  has elapsed, and the crystals then grow for a shorter time  $t_c$ .

The throughput  $r_c$  in Eq. (8) can be replaced by using Eq. (10), whereby the relation

$$L_m^{(1+3i)} = 3B_N m_c^{(1-d)} (t_c/3)^{(1-d)} \quad (11)$$

is obtained for discontinuous crystallization. A procedure based on linearization of Eq. (11) has been suggested<sup>6</sup> for determining the kinetic coefficients  $i$  and  $d$ .

The "mean" rates of nucleation and growth can be calculated from the granulometric composition of products from discontinuous model experiments as follows<sup>4</sup>:

$$B^0 = 27m_c / (2\alpha Q_c L_m^3 t_s) \quad (12)$$

$$G = L_m / t_c \quad (9)$$

Supersaturation in a batch experiment usually is not constant. If an unseeded solution is supersaturated, it increases first rapidly and, after the formation of the first crystal nuclei, it exhausts gradually due to their growth. This is associated with changes in the instantaneous nucleation and growth rates. Unfortunately, no reliable method exists for continuous measurement of very low supersaturations in suspensions. The "instantaneous" rates were therefore estimated by using the relations

$$B^0 = 27\Delta m_c / (2\alpha Q_c L_m^3 \Delta t_s) \quad (13)$$

$$G = \Delta L_m / \Delta t_c \quad (14)$$

where the differences of the quantities measured refer to experiments differing only in the  $t_s$  times.

## EXPERIMENTAL

Evaporation and cooling were accomplished in the same crystallizer, constituted by a closed 2.5 l glass vessel with a half-spherical bottom and a two-blade stirrer; the stirring rate was 10 rps<sup>7</sup>.

Each experiment was performed with 1 000 g of distilled water and 842 g of high-purity ammonium aluminium sulfate dodecahydrate (impurity content lower than 0.05 wt. %). This

component ratio corresponds to a saturation temperature of 70.0°C (ref.<sup>8</sup>). The sulfate was dissolved at 72°C, and the solution was cooled to 70°C and thermostatted for 30 min.

During the evaporation crystallization, the solution was brought to boil at a reduced pressure. For the entire evaporation period, the temperature was held at 70°C by means of pressure control. The solvent vapours condensed in a reflux condenser; a fraction of the condensate was fed to the receiver at a constant rate, the remaining fraction was brought back to the crystallizer. Two rates were used for taking off the condensate and thus for the solution supersaturation. At the adjusted rate, the experiments were terminated after taking off different amounts of condensate.

During the cooling crystallization the cooling via the vessel jacket was controlled so that the supersaturation rate was comparable to that in the previous experiments, where the supersaturation rate was nonlinear at a linear rate of the solvent offtake. The cooling obeyed the equation

$$T = 70 - (70 - T_c) (t/t_s)^X \quad (15)$$

where  $X = 1.75$  for the series of experiments comparable to a faster evaporation, and  $X = 1.90$  for slower evaporation. The final temperature of cooling  $T_c$  was chosen so that the suspension concentrations  $m_c$  approached those attained during the evaporation.

After reaching the final conditions, the crystals were filtered out, dried at room temperature, and subjected to sieve analysis.

## RESULTS AND DISCUSSION

The experiments are divided into four groups with respect to the supersaturation procedure and rate (Table I). Each group comprises several experiments with different crystallization times  $t_s$ .

Arrangement of the experiments by increasing  $t_s$  shows the development of the particle size distributions in the given saturation procedure. This is demonstrated in Figs 1 and 4. It is evident that the product from the cooling crystallization exhibits a lower dispersion about the mean value and is more homogeneous than the product from the evaporation. This can be explained so that several nucleation waves of similar intensity occurred during the evaporation, whereas a single nucleation took place during the cooling.

The time behaviour of the nucleation rate (13) and growth rate (14) is shown in Figs 5 and 6, respectively. The number of points in the plots is insufficient to prove the above hypothesis concerning the repeated nucleation. To a degree, however, the plots demonstrate that the nucleation and growth rates depend on the supersaturation (5), (6), and follow its course.

The kinetic equation exponent ratio  $g/n$  and other constants were obtained by solving Eq. (11) for sets differing in the way of supersaturation. The data are given in Table II.

Table I gives the relative percentage differences between the experimental and calculated mean particle size values,

$$p = 100 \cdot |L_{m,exp} - L_{m,calc}| / L_{m,exp} \quad (16)$$

where  $L_{m,calc}$  values were obtained from Eq. (11) using constants given in Table II.

The fit of the model was tested by means of the correlation coefficient  $r$  for two

TABLE I  
Observed and calculated parameters

Saturation procedure	$t_s$ s	$t_c$ s	$m_c$ kg kg <sup>-1</sup>	$L_{m,exp}$ 10 <sup>-3</sup> m	$L_{m,calc}$ 10 <sup>-3</sup> m	$p$ %	$G \cdot 10^{10}$ m s <sup>-1</sup>	$B^0$ kg <sup>-1</sup> s <sup>-1</sup>
Evaporation								
slow	6 048	3 360	0.043	0.739	0.804	9	1 330	239
	12 486	8 400	0.146	0.945	0.901	5	192	382
	15 831	11 760	0.191	0.867	0.963	11	185	263
	16 838	11 700	0.240	1.042	0.932	11	94	466
	20 739	15 120	0.300	1.048	0.978	7	135	316
fast	1 384	420	0.056	0.450	0.410	9	9 760	10 260
	3 123	1 260	0.157	0.488	0.499	2	1 060	8 170
	4 160	3 000	0.221	0.583	0.621	6	700	4 500
	5 057	2 940	0.265	0.576	0.603	5	620	4 450
	5 729	3 780	0.304	0.602	0.639	6	430	3 890
Cooling								
slow	12 150	5 850	0.160	0.522	0.505	3	860	1 790
	15 300	8 820	0.211	0.532	0.553	4	162	1 670
	17 700	11 040	0.254	0.585	0.587	0	153	1 550
	20 400	14 010	0.300	0.626	0.620	1	108	1 250
fast	3 240	1 500	0.176	0.420	0.426	1	2 840	12 280
	4 020	2 160	0.226	0.457	0.463	1	560	11 290
	4 540	2 580	0.257	0.488	0.477	2	333	10 400
	5 700	3 900	0.311	0.519	0.520	0	326	5 790

TABLE II  
Constants in equation (11)

Constant	Evaporation	Cooling
$i$	0.36 ± 0.03	0.61 ± 0.01
$d$	1.7 ± 0.3	0.4 ± 0.1
$B_N \cdot 10^{10}$	5.5 ± 0.9	0.16 ± 0.01
$r$	0.96	0.98

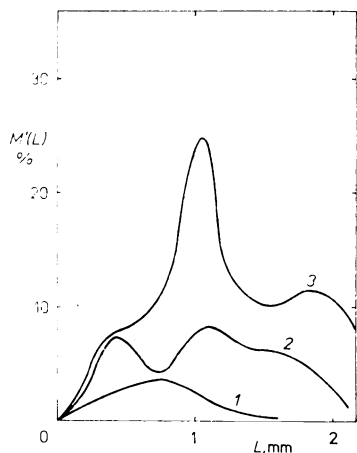


FIG. 1

Time development of differential granulometric composition of crystals during saturation by slow cooling. Final solid fraction  $m_c$  ( $\text{kg kg}^{-1}$ ) in the suspension: 1 0.05, 2 0.15, 3 0.30

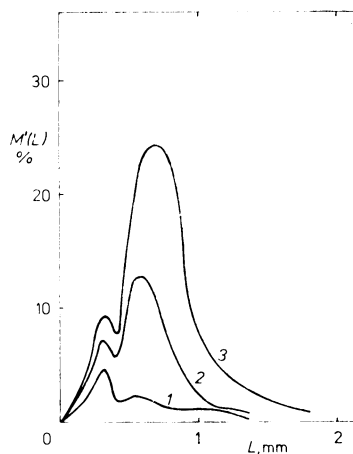


FIG. 2

Time development of differential granulometric composition of crystals during saturation by fast cooling. Curve labelling as in Fig. 1

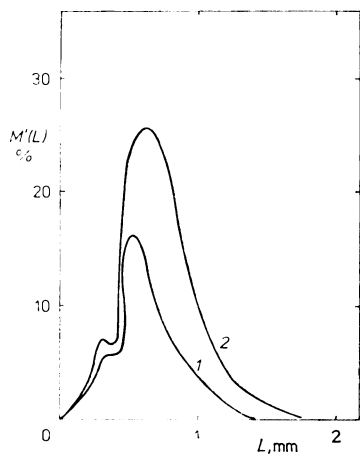


FIG. 3

Time development of differential granulometric composition of crystals during saturation by slow evaporation. Final solid fraction  $m_c$  ( $\text{kg kg}^{-1}$ ) in the suspension: 1 0.15, 2 0.30

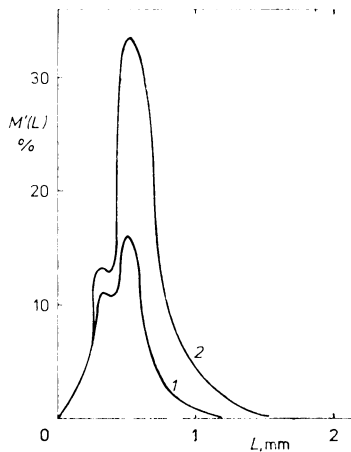


FIG. 4

Time development of differential granulometric composition of crystals during saturation by fast evaporation. Curve labelling as in Fig. 3

data sets<sup>9</sup> (according to the way of supersaturation):

$$1 - r^2 = \frac{\sum(L_{m,exp,j} - L_{m,calc,j})^2}{\sum(L_{m,exp,j} - S)^2} \quad (17)$$

where  $S$  is the arithmetic mean of the measured mean crystal size values  $L_{m,exp,j}$  in the given data set. The correlation coefficient values are given in Table II. In no

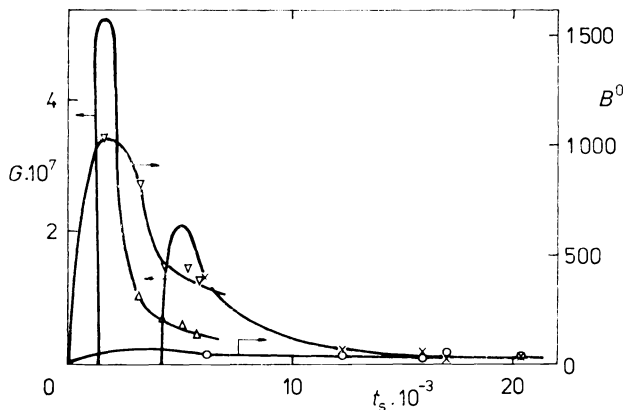


FIG. 5

Time behaviour of the nucleation rate  $B^0$  ( $\circ$ ,  $\nabla$ ) and of the linear growth rate  $G$  ( $\times$ ,  $\Delta$ ) during saturation by slow ( $\circ$ ,  $\times$ ) and fast ( $\nabla$ ,  $\Delta$ ) cooling

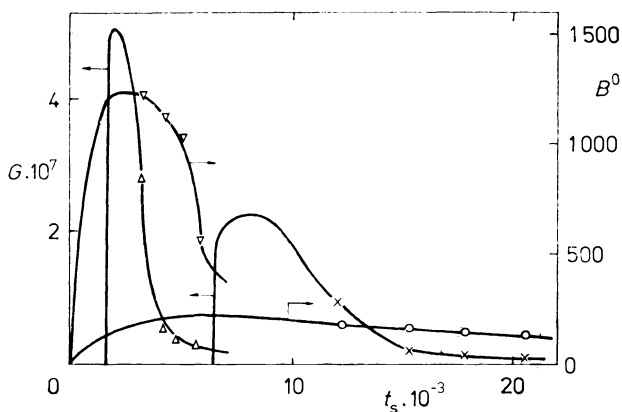


FIG. 6

Time behaviour of the nucleation rate  $B^0$  ( $\circ$ ,  $\nabla$ ) and of the linear growth rate  $G$  ( $\times$ ,  $\Delta$ ) during saturation by slow ( $\circ$ ,  $\times$ ) and fast ( $\nabla$ ,  $\Delta$ ) evaporation

case the difference between the experimental and calculated crystal size values is statistically significantly different, and so the model relation (11) can be considered suitable for the two supersaturation procedures.

The differences for any of the parameters examined are significant. The system constant  $B_N$  is defined so that it respects the course of the process; therefore the different values do not surprise. The nucleation is considerably more intensive in the evaporation procedure, which can be attributed, among other things, to the occurrence of a higher number of concentration inhomogeneities induced by the boil, which can bring about higher local supersaturation in the sites of formation of bubbles.

The relative growth and nucleation exponent  $i = 0.61$  for the cooling is in a very good agreement with previous measurements performed in a different cooling crystallizer in different hydrodynamic conditions, and also in agreement with the value obtained by separate measurement of the nucleation and growth. The  $i$  value obtained during the evaporation was entirely different. The two processes differ particularly in the nucleation rate, as evidenced by the  $B^0$  values (Table I) as well as by the time required for the first crystals to form. The mean values of these intervals are 4 250 and 6 435 s for slow evaporation and cooling, respectively, and 1 611 and 1 840 s for fast evaporation and cooling, respectively. In contrast to nucleation, the differences in the growth rates are not statistically significant.

Based on these results we suggest that the evaporation and cooling crystallization procedures differ primarily in the rate of nucleation. The higher rate of nucleation in the boiling solution can be explained in terms of local increase in supersaturation in sites of formation of solvent vapour bubbles, as well as in terms of more intensive secondary nucleation in the suspension which is stirred not only by the stirrer but also by the forming bubbles, owing to which collisions of the crystals present are more frequent. This also follows from the observed secondary nucleation coefficient values, viz.  $d = 1.7$  in the evaporation and  $d = 0.4$  in the cooling modes.

Since nucleation proceeds sooner in the evaporation mode, the crystals can grow for a longer period of time in comparable experiments. This can account for the larger crystal size.

The significant differences in the kinetic parameters of crystallization for the evaporation and cooling modes bear out the well-known empiric fact that in measuring kinetic data for designing the crystallization equipment, it is particularly the same way of solution supersaturation that, in addition to a number of other conditions, must be adhered to.

#### SYMBOLS

$B^0$	numerical nucleation rate, $\text{kg}^{-1} \text{s}^{-1}$
$B_N$	system kinetic constant of crystallization



$d$	secondary nucleation exponent
$G$	linear rate of crystal growth, $\text{m s}^{-1}$
$g$	kinetic order of growth rate
$i$	relative kinetic exponent ( $= g/n$ )
$j$	experiment No.
$k'_G$	growth rate constant, $\text{m s}^{-1}$
$k'_N$	nucleation rate constant, $\text{kg}^{-1} \text{s}^{-1}$
$L$	particle size, $\text{m}$
$L_m$	mean particle size, $\text{m}$
$M(L)$	cumulative mass distribution function of particle size, %
$M'(L)$	differential mass distribution function of particle size, %
$m_c$	solid phase mass fraction in suspension, $\text{kg kg}^{-1}$
$n$	kinetic order of nucleation rate
$p$	difference between experimental and calculated data, %
$r$	correlation coefficient
$r_c$	crystallization rate, $\text{kg s}^{-1}$
$S$	arithmetic mean of experimental data, $\text{m}$
$t$	time of cooling, $\text{s}$
$t_c$	time of crystal growth, $\text{s}$
$t_1$	mean residence time of solution in crystallizer, $\text{s}$
$t_s$	total time of supersaturation, $\text{s}$
$T$	temperature, $^{\circ}\text{C}$
$T_e$	final temperature of cooling, $^{\circ}\text{C}$
$\Delta w$	supersaturation, $\text{kg kg}^{-1}$
$z$	dimensionless particle size
$\alpha$	volume shape coefficient
$\rho_c$	crystal density, $\text{kg m}^{-3}$

## REFERENCES

1. Hložný L., Broul M. in: *Industrial Crystallization '87* (J. Nývlt and S. Žáček, Eds), p. 571. Elsevier, Amsterdam 1989.
2. Randolph A. D., Larson M. A.: *Theory of Particulate Processes*. Academic Press, New York 1971.
3. McCabe W. L.: *Ind. Eng. Chem.* 21, 30 (1929).
4. Nývlt J., Söhnel O., Matuchová M., Broul M.: *The Kinetics of Industrial Crystallization*. Elsevier, Amsterdam 1985.
5. Broul M.: *Thesis*. Prague Institute of Chemical Technology, Prague 1979.
6. Hložný L., Broul M. in: *Industrial Crystallization '90* (A. Mersmann, Ed.), p. 491. VDI Verlag München, Garmisch-Partenkirchen 1990.
7. Broul M., Provazník L., Procházka S., Šůra J., Nývlt J.: *Chem. Listy* 68, 431 (1974).
8. Broul M., Nývlt J., Söhnel O.: *Solubility in Inorganic Two-Component Systems*. Elsevier, Amsterdam 1981.
9. Janko J.: *Statistické tabulky*. Nakladatelství ČSAV, Praha 1958.

Translated by P. Adámek.